J Mater Sci (2007) 42:7069–7075
DOI 10.1007/s10853-007-1536-7

Characterizing the surface properties of carbon nanotubes by inverse gas chromatography

Xiali Zhang · Dong Yang · Peng Xu · Changchun Wang · Qiangguo Du

Received: 29 July 2006 / Accepted: 19 January 2007 / Published online: 5 May 2007

Abstract Inverse gas chromatography (IGC) was used to characterize the surface properties of pristine multi-walled carbon nanotubes (MWNTs), as well as the poly(acrylic acid) sidewall covalently functionalized MWNTs (PAA-g-MWNTs) and hydroxyl group directly grafted MWNTs (MWNTols). The dispersive component of the surface energy (γ_S^D) and the acid/base character of these samples' surfaces were estimated by the retention time with different non-polar and polar probes at infinite dilution region. The specific free energy (ΔG^{AB}) and the enthalpy (ΔH^{AB}) of adsorption corresponding to acid–base surface interactions were determined. By correlating ΔH^{AB} with the donor and acceptor numbers of the probes, the acidic (K_A) and the basic K_D parameters of the samples' were calculated. The results show that chemical modification successfully reduces the dispersive component of the surface energy of MWNTs. Furthermore, MWNTs grafted with hydroxyl groups exhibit a more basic character, while MWNTs grafted with poly(acrylic acid) show a more acidic character. Overall, IGC provides useful complementary information on the changes resulted from the chemical modifications of the surface.

X. Zhang · D. Yang · P. Xu · C. Wang · Q. Du (✉)
Key Laboratory of Molecular Engineering of Polymers of Ministry of Education, Department of Macromolecular Science, Fudan University, Shanghai 200433, China
e-mail: qgdu@fudan.edu.cn

C. Wang (✉)
e-mail: ccwang@fudan.edu.cn

Introduction

Since their discovery [1], carbon nanotubes (CNTs) have attracted tremendous interest due to their unique chemical and physical properties, such as high aspect ratios, good elasticity, extremely high Young's modulus, and high conductivity of electricity and heat [2–4]. CNTs are perceived as an ideal reinforcing material for composites and considerable studies on CNTs/polymer composites have been reported [5–7]. However, due to the poor compatibility with polymer and the strong Vander Waals forces among tubes, CNTs tend to agglomerate and form bundles in composites, which jeopardizes the properties of the composites [8]. It is suggested that the dispersibility of CNTs in polymer matrix and the interfacial bonding between CNTs and polymer are the key factors to realize the nano-reinforcement of composites.

The chemical functionalization of CNTs can effectively improve CNTs' dispersibility and compatibility in polymer matrix [9–11]. Several methods were employed to characterize the chemical functionalized CNTs, such as FT-IR, NMR, Raman, AFM and TGA etc. [12–14]. However, all the above methods cannot give adequate information about the CNT's surface properties, which is much important in the research of CNT/polymer composites. Therefore, development of an adequate method that can quantitatively characterize the surface properties of CNTs before and after functionalization is highly required and yet a challenging work.

Inverse gas chromatography (IGC) is a powerful technique for investigating the characteristics of solid surfaces in powder form [15] and has been widely used to the characterizing of the surface properties of calcium carbonate, fibers, clays, polymers, fullerene, graphite, and carbon black etc. [16–20]. Herein, we used IGC to deter-

mine the surface thermodynamic characteristics of multi-walled carbon nanotubes (MWNTs) and their derivatives, by using different probe molecules under the condition of near zero surface coverage of the test materials.

Theory

Inverse gas chromatography is widely used to characterize the surface properties of organic and inorganic materials. The difference between IGC and conventional gas chromatography (GC) is that for IGC the interest is the solid material packed in the column instead of the injected vapor and the vapors used as probes are of known properties.

The retention times of saturated *n*-alkanes and acid–base probes at infinite dilution can be used to calculate the dispersive component (γ_S^D) of the surface energy, the specific free energy of adsorption (ΔG^{AB}), and the enthalpy of adsorption (ΔH^{AB}) corresponding to acid–base surface interactions. Papirer's approach, as described by Schultz and colleagues [21], was used to estimate the acceptor (K_A) and donor (K_D) parameters of the test substrates.

The primary measurement in IGC is the net retention volume, V_N, which can be calculated according to the following equation [22, 23],

$$V_N = Fj(t_R - t_M)\left(\frac{p_0 - p_w}{p_0}\right)\left(\frac{T_C}{T_{meter}}\right) \quad (1)$$

where F is the flow rate, t_R and t_M are the retention and dead times measured with a specific probe and a non-adsorbing probe (such as methane) respectively, p_0 is the pressure at the flow meter, p_w is the vapor pressure of pure water at the temperature of the flow meter (T_{meter}), and T_c is the column temperature. j is the James-Martin factor for the correction of gas compressibility when the column inlet (P_i) and outlet (P_o) pressures are different and it is given by

$$j = \frac{3}{2}\left[\frac{(p_i/p_0)^2 - 1}{(p_i/p_0)^3 - 1}\right] \quad (2)$$

The interaction of neutral probes, such as saturated *n*-alkanes, with the substrate material is predominated by van der Waals dispersive forces. It has been shown that at infinite dilution of the injected probe vapor, the dispersive component γ_S^D of the total surface energy of the substrate is related to V_N by the following equation,

$$RT_C \ln V_N = 2N(\gamma_S^D)^{1/2}\alpha(\gamma_L^D)^{1/2} + C^t \quad (3)$$

where R is the gas constant, T_C is the column absolute temperature, N is Avogadro's number, α is the surface area of the probe molecule, γ_L^D is the dispersive component of the surface energy of the probe, and C^t is a constant. The plot of $RT_c \ln V_N$ versus $2N\alpha(\gamma_L^D)^{1/2}$ should give a straight line with the slope $(\gamma_S^D)^{1/2}$.

The interactions between polar probes and the substrate involve both dispersive and specific interactions. And the specific interactions include dipole–dipole and acid–base interactions (or the electron acceptor–donor effect), the latter involving much higher energy than the former. In fact, it is usually assumed that the specific contributions of the adsorption of polar probes are solely from acid–base interactions. The free energy of adsorption, ΔG^{AB}, corresponding to acid–base surface interactions is related to V_N by the following equation,

$$-RT \ln(V_N/V_N^{ref}) = \Delta G^{AB} \quad (4)$$

where V_N is the specific retention volume of a polar probe and V_N^{ref} is the specific retention volume of a hypothetical reference *n*-alkane with the same $2N\alpha(\gamma_L^D)^{1/2}$ value as the polar probe.

The difference in the ordinates between the points corresponding to the specific polar probe and the reference gives an estimate of the free energy of adsorption corresponding to the polar probe's specific acid–base interactions with the substrate.

The free energy of adsorption, ΔG^{AB}, corresponding to the specific acid–base interactions is also related to the enthalpy of adsorption, ΔH^{AB} by the following equation,

$$\Delta G^{AB} = \Delta H^{AB} - T\Delta S^{AB} \quad (5)$$

where ΔS^{AB} is the entropy of adsorption corresponding to the specific acid–base interactions. A plot of $\Delta G^{AB}/T$ versus $1/T$ should yield a straight line with slope ΔH^{AB}. The enthalpy of adsorption corresponding to the specific acid–base interaction, ΔH^{AB}, is related to the surface acceptor and donor parameters, K_A and K_D, of the substrates by the following expression,

$$-\Delta H^{AB} = K_A DN + K_D AN \quad (6)$$

where DN and AN are the numbers of donors and acceptors, respectively, of the acid–base probe as defined by Gutmann. A plot of ΔH^{AB}/AN versus DN/AN should yield a straight line with slope K_A and intercept K_D.

Experimental and methods

Materials

The MWNTs produced by chemical vapor deposition (CVD) method, were purchased from Sun Nanotech Co.

Ltd (Nanchang, China). The purity of the MWNTs is ~90%. The pristine MWNTs were purified according to Ref. [24]. MWNTs modified with hydroxyl groups (MWNTols) and poly(acrylic acid) (PAA-g-MWNTs) were prepared in our laboratory [25, 26]. *n*-Pentane, *n*-hexane, *n*-heptane, *n*-octane, nonane, dichloromethane (DCM), ethyl acetate (EtAc), acetone (Acet), tetrahydrofuran (THF) and diethylether (DEE) (analytical reagent grade) were purchased from Shanghai Chemical Reagents Company and Shanghai Lingfeng Chemical Reagent Co., Ltd., and used as received. Their physiochemical properties are listed in Table 1. The donor numbers (DN) and acceptor numbers (AN) of the probes were taken from literatures [21, 27, 28]. These probes are commonly used in IGC for solid surface characterization.

Characterization

FT-IR, TEM and TGA were used for the characterization of pristine MWNTs, MWNTols and PAA-g-MWNTs. FT-IR analyses were recorded on a Nexus-470 FTIR spectrophotometer (Nicolet Instruments, USA). Transmission electron micrographs were obtained using a HITACHI H-600 electron microscope operated at an acceleration voltage of 100 kV. The powder samples of MWNTs (or derivatives) were fully dispersed in distilled water and a drop of the dispersion was deposited on a carbon-coated copper grid, and water was allowed to evaporate. Thermogravimetric analysis (TGA) measurements were performed on a Perkin-Elmer Pyris 1 under nitrogen atmosphere from 50 °C to 800 °C at a ramp of 10 °C min^{-1}.

Inverse gas chromatography

The chromatographic experiments were performed with a (GC112A) gas chromatography equipped with a flame ionization detector. Retention times were recorded on a (N2000) workstation.

Nitrogen with high purity (99.999%) was used as the carrier gas with a flow rate of about 30 mL min^{-1}. The flow rate of the carrier gas was measured at the detector outlet with a soap bubble flow-meter and was corrected for the pressure drop and the temperature change in the column using the James-Martin factor.

A stainless steel column (30 cm long, 2 mm i.d.), cleaned with methanol and acetone, was used in this study. About 0.2 g of sample was filled into the column via the aid of vacuum and mechanical vibration. The two ends of the column were plugged with silane-treated glass wool. The column was then stabilized in the GC system at 57 °C overnight with a nitrogen flow at the rate of 30 mL min^{-1}. In order to avoid contaminating the detector, the outlet of the column was not connected to the detector during this stabilization treatment period.

Measurements were carried out in the temperature range of 37–57 °C. In order to meet the requirement of adsorption at infinite dilution, corresponding to zero coverage and GC linearity, the probes were introduced into the column using a 1 μL syringe with injecting vapor volume less than 0.1 μL. Therefore, the solute–solute interaction is infinitesimal and can be neglected, and the retention on the solid surface can be regarded as governed solely by solid–probe interactions. For each measurement, at least three repeated injections were made to obtain reproducible results. Methane was used as the marker for the retention time correction and it was used to ensure the absence of dead volume when a new column was placed in the chromatographic system.

Results and discussion

FT-IR, TEM and TGA characterization of MWNTs and their derivatives

The FT-IR spectra of pristine MWNTs, MWNTols and PAA-g-MWNTs are shown in Fig. 1. For pristine MWNTs, there is no obvious signal in the FT-IR spectrum (Fig. 1a).

Table 1 Physicochemical properties of the IGC probes used in the present study

Probe	α (Å)^2	γ_L^D (mJ m^{-2})	AN (kJ mol^{-1})	DN (kJ mol^{-1})	Specific character
n-Pentane	45.0	16.1	–	–	Neutral
n-Hexane	51.5	18.4	–	–	Neutral
n-Heptane	57.0	20.3	–	–	Neutral
n-Octane	62.8	21.3	–	–	Neutral
n-Nonane	69.0	22.7			Neutral
DCM	31.5	27.6	16.3	0	Acid
EtAc	48.0	19.6	6.3	71.5	Amphoteric
Acet	42.5	16.5	10.5	71.1	Amphoteric
THF	45.0	22.5	2.1	84.0	Base
DEE	47.0	15.0	5.9	80.6	Base

After chemically functionalized, the peak of O–H stretching vibration at 3,427 cm^{-1} was clearly observed in the FT-IR spectrum of MWNTols (Fig. 1b). For PAA-g-MWNTs, the stretch absorption peaks of C=O and O–H for the carboxyl (COOH) at 1,707 cm^{-1} and 3,432 cm^{-1} can be clearly observed, and the peaks at 2,900 to 3,100 cm^{-1} are attributed to the C–H stretching vibration.

The TEM images of MWNTols (Fig. 2b) and PAA-g-MWNTs (Fig. 2c) are similar to that of pristine MWNTs (Fig. 2a), which indicates that the process of chemical functionalization did not destroy the tube structures. It is notable that although MWNTols and PAA-g-MWNTs were both well dispersed, the diameters of PAA-g-MWNTs were clearly larger than those of MWNTols and MWNTs. It may be due to the enwrapment of poly(acrylic acid) onto CNTs' surface, which increased the efficient diameter of CNTs. For MWNTols, hydroxyl groups preferably improved the dispersibility of the nanotubes but had little effect on the tubes' diameter. The hypothesis is also supported by TGA results (Fig. 3).

As shown in Fig. 3, the TGA result of pristine MWNTs shows neglectable weight loss from 50 °C to 800 °C under nitrogen atmosphere. And MWNTols shows a little more weight loss than pristine MWNTs. PAA-g-MWNTs shows two weight loss regions at 180–270 °C and 320–450, corresponding to the decomposition of carboxyl and alkane units respectively, and the total weight loss is about 40%.

IGC characterization of MWNTs and their derivatives

Influence of the carrier gas flow rate on measurements

Literature data show that flow rates used for IGC measurements can be very different (from 7 mL/min to 35 mL/min) [29]. Planinsek et al. [30] have shown that the flow rate does not affect the surface energy when using a range of pharmaceutical powders in IGC. However, the flow rate may affect the results for carbon nanotubes. For example, it is possible that probes can diffuse into tube and therefore it is interesting to study the influence of flow rate. The variation of retention volume of alkanes is shown in Fig. 4 as a function of the carrier gas flow rate with PAA-g-MWNTs as stationary phases at 330.2 K. It can be observed that the retention data were independent of the carrier gas flow rate in both instances, which indicates that the measurements are not limited by diffusion effects.

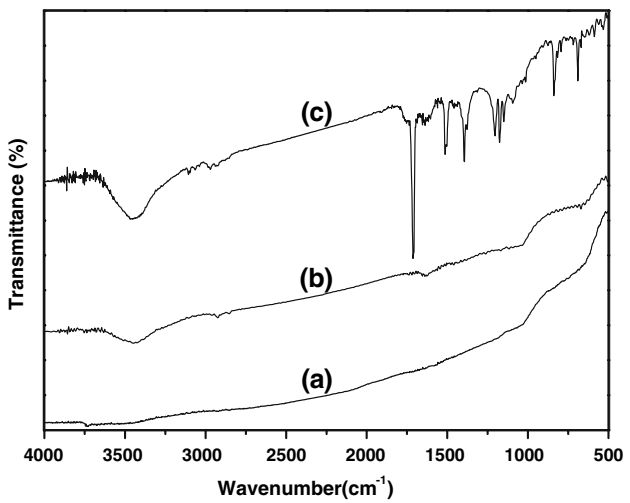

Fig. 1 FT-IR spectra of (**a**) pristine MWNTs, (**b**) MWNTols and (**c**) PAA-g-MWNTs

Dispersive component of the surface energy

The dispersive component of the surface energy of the solid, γ_S^D, provides the information of the force field of the high-energy sites. According to general knowledge, γ_S^D is proportional to the surface density of the atoms, their polarizability, and their ionization energy [31]. The dispersive component of the surface energy, γ_S^D, calculated according to Eq. 3 are presented in Table 2. The measured value of the surface free energy is about 120 mJ m^{-2} for MWNTs at 315.2 K, which is much higher than that for fullerene (57.8 mJ m^{-2} at 312 K), but lower than those for graphite (279 mJ m^{-2} at 416 K) and carbon black (174.1 and 204.1 mJ m^{-2} at 453 K) observed by Papirer et al. [20]. The impurities on the surface of fullerene and CNTs, induced by the carbon atom of the defect during purification process, resulted in lower γ_S^D values than those of carbon black and graphite. In comparison with fullerene, CNTs has lower ratio of the C of the defect and hence the higher γ_S^D value and lower activity.

The grafting of poly(acrylic acid) or hydroxyl groups onto the surface of CNTs resulted in the reduction of γ_S^D values (Table 2). And the effect is significantly greater when grafted with poly(acrylic acid) which agrees with the results of TEM and TGA. The γ_S^D value of PAA-g-MWNTs (38 mJ m^{-2} at 325.2 K) is close to those of calcium carbonates coated with sodium polyacrylate (40 mJ m^{-2} at 343 K) observed by Price and Ansari [16] and (30–35 mJ m^{-2} at 333 K) by Shui [32]. It is also similar to the values of polyolefins (around 30–35 mJ m^{-2}) measured by other techniques [33]. This reduction of γ_S^D values were caused by the poly(acrylic acid) chain wrap CNTs' surface for PAA-g-MWNTs or hydroxyl groups grafted for MWNTols. For MWNTols, only some hydroxyl groups are grafted onto the surface of CNTs, therefore, the γ_S^D values of MWNTols are still close to those of MWNTs.

Acid–base nature of the surfaces

Polar probes were used for the investigation of the acid–base nature of the surfaces. The free energy of the

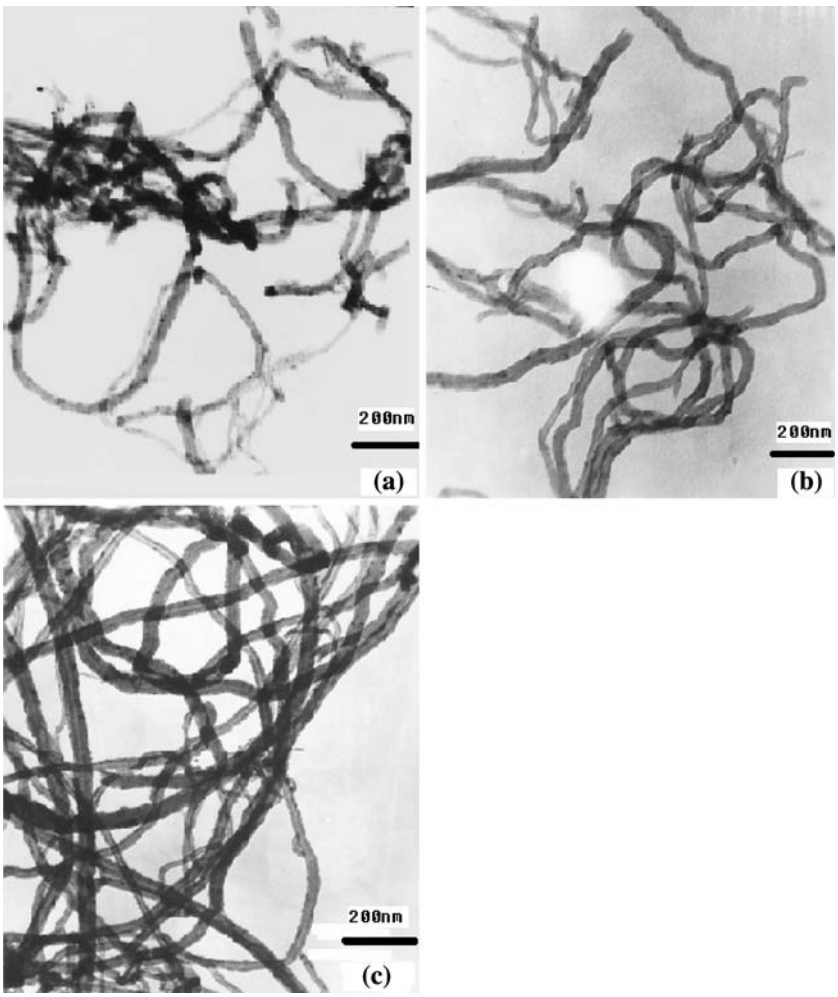

Fig. 2 TEM images of (**a**) pristine MWNTs, (**b**) MWNTols and (**c**) PAA-g-MWNTs

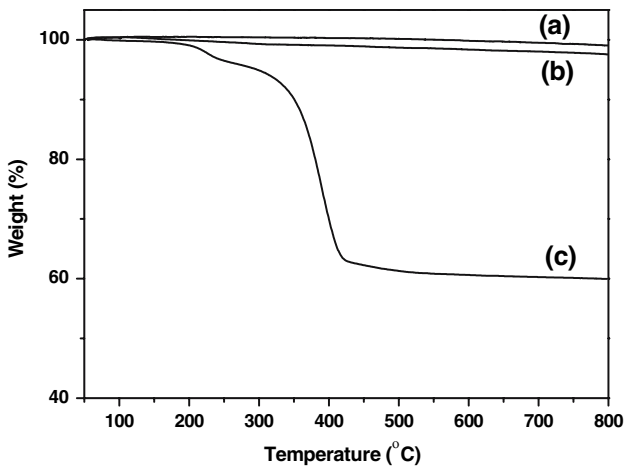

Fig. 3 TGA curves of (**a**) Pristine MWNTs, (**b**) MWNTols and (**c**) PAA-g-MWNTs

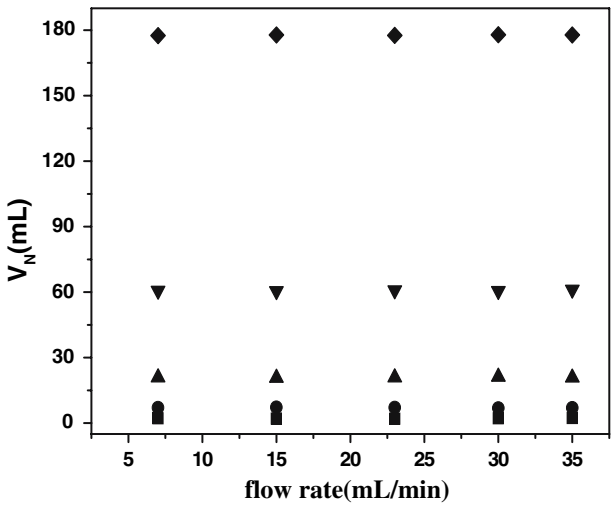

Fig. 4 Influence of carrier gas flow rate on the retention volume at 330.2 K for pentane (■), hexane (●), heptane (▲), octane (▼) and nonane (♦) over PAA-g-MWNTs

Table 2 Dispersive component, γ_S^D, of the surface energy of pristine MWNTs and the derivatives at different temperatures

T/K	γ_S^D/(mJ m^{-2})		
	Pristine MWNTs	PAA-g-MWNTs	MWNTols
310.2	122.98	41.32	109.60
315.2	120.87	40.12	107.99
320.2	118.18	39.53	105.66
325.2	116.20	38.00	103.18
330.2	114.04	37.42	102.31

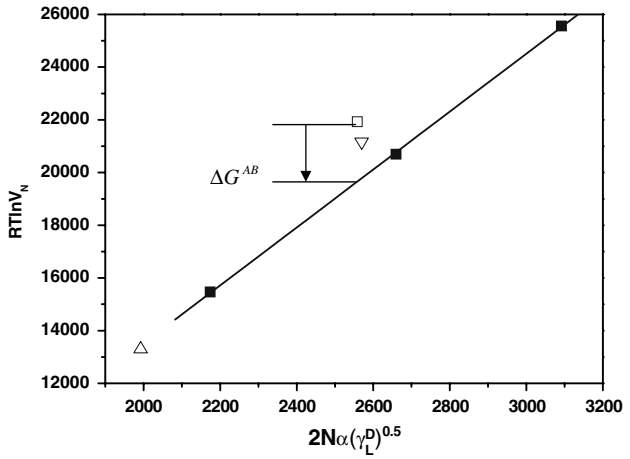

Fig. 5 Determination of ΔG^{AB} for polar probes on MWNTs at 315.2 K (■ alkane Δ DCM, □ EtAc, ∇ THF)

Table 4 The specific enthalpy of adsorption (ΔH^{AB}) of polar probes on pristine MWNTs and the derivatives

Probe	$-\Delta H^{AB}$ (kJ mol^{-1})		
	Pristine MWNTs	PAA-g-MWNTs	MWNTols
DCM	0.890(0.996)	3.56(0.996)	7.13(0.988)
EtAc	6.20(0.992)	13.41(0.986)	9.91(0.984)
Acet	7.40(0.983)	13.33(0.999)	13.56(0.973)
THF	7.82(0.997)	16.67(0.995)	11.35(0.992)
DEE	7.43(0.960)	15.57(0.998)	9.22(0.988)

Regression coefficients (R^2) are given in parentheses

Table 5 Surface acceptor and donor parameters K_A and K_D for MWNTs and derivatives

Probe	Pristine MWNTs	PAA-g-MWNTs	MWNTols
K_A	0.091	0.195	0.125
K_D	0.027	0.025	0.255
K_D/K_A	0.299	0.128	2.040
$(R^2)^a$	0.998	0.998	0.983

[a] Regressive coefficients

acid–base interactions of polar probes with the samples, ΔG^{AB}, was calculated according to Eq. 4. An example of the plot for MWNTs at 315.2 K is shown in Fig. 5.

Table 3 shows the free energy of the specific interactions between the three samples and polar probes at

Table 3 The specific free energy of adsorption ΔG^{AB} of polar probes on pristine MWNTs and the derivatives at different temperatures

Substrate/Probe	$-\Delta G^{AB}$ (kJ mol^{-1})				
	310.15 K	315.15 K	320.15 K	325.15 K	330.15 K
Pristine MWNTs					
DCM	–0.122(0.004)	–0.140(0.005)	–0.158(0.005)	–0.174(0.004)	–0.187(0.004)
EtAc	2.310(0.020)	2.259(0.014)	2.190(0.020)	2.130(0.016)	2.068(0.018)
Acet	5.530(0.008)	5.501(0.009)	5.482(0.005)	5.440(0.012)	5.412(0.008)
THF	1.601(0.027)	1.483(0.036)	1.372(0.019)	1.284(0.029)	1.171(0.020)
DEE	0.952(0.021)	0.830(0.025)	0.783(0.019)	0.590(0.028)	0.550(0.021)
PAA-g-MWNTs					
DCM	1.582(0.002)	1.541(0.006)	1.514(0.007)	1.483(0.006)	1.454(0.005)
EtAc	7.398(0.018)	7.310(0.016)	7.171(0.021)	7.105(0.022)	7.024(0.030)
Acet	5.823(0.007)	5.703(0.005)	5.585(0.005)	5.450(0.008)	5.341(0.007)
THF	8.154(0.018)	8.023(0.023)	7.830(0.022)	7.684(0.009)	7.551(0.025)
DEE	6.295(0.019)	6.152(0.023)	6.011(0.026)	5.830(0.013)	5.702(0.025)
MWNTols					
DCM	–0.803(0.009)	–0.962(0.009)	–1.044(0.004)	–1.221(0.008)	–1.311(0.009)
EtAc	3.852(0.011)	3.791(0.010)	3.711(0.019)	3.623(0.013)	3.502(0.012)
Acet	4.603(0.009)	4.502(0.008)	4.380(0.005)	4.120(0.010)	4.061(0.009)
THF	1.910(0.020)	1.719(0.020)	1.678(0.018)	1.451(0.020)	1.298(0.025)
DEE	2.145(0.015)	2.033(0.023)	1.891(0.022)	1.831(0.018)	1.682(0.022)

Standard deviations are given in parentheses

different temperatures. It can be observed that for PAA-g-MWNTs, probes with large DN number (such as THF) show higher ΔG^{AB} values, which suggests that the surface of PAA-g-MWNTs is acidic. For pristine MWNTs and MWNTols, amphoteric probes exhibit higher ΔG^{AB} values, which implies that their surfaces are amphoteric. For pristine MWNTs, its amphoteric surface property may be caused by –OH and –COOH produced during the purification process.

The values of the specific enthalpy of adsorption, ΔH^{AB}, computed by varying $\Delta G^{AB}/T$ against $1/T$ according to Eq. 5, are shown in Table 4. By plotting $-\Delta H^{AB}/AN$ versus DN/AN according to Eq. 6, K_A and K_D can be obtained from the slope and the intercept, respectively. The values of K_A and K_D are listed in Table 5. The amphoteric characteristics of pristine MWNTs and MWNTols is reflected in the K_D/K_A ratio. It can be seen from Table 5 that MWNT's surface is predominantly acidic while MWNTols' is basic.

Conclusions

Inverse gas chromatography was used to characterize the surfaces of pristine MWNTs, PAA-g-MWNTs and MWNTols at infinite dilution. Chemical modification has successfully reduced the dispersive component of the surface energy of MWNTs, as measured by the dynamic adsorption of *n*-alkanes. The acid–base character of MWNTs' surface was adjusted by surface modification. MWNTs grafted with hydroxyl groups exhibit a more basic character, while MWNTs grafted with poly(acrylic acid) show a more acidic character. Overall, the results showed that IGC is an effective method to characterize the changes in CNTs' surface properties especially when combined with additional techniques such as FT-IR, TEM and TGA analysis. And it provides useful complementary information on the changes resulted from the chemical modifications of the surface.

Acknowledgements This work was supported by National Science Foundation of China (Grant No.20374012), National Science Foundation for Distinguished Yong Scholars of China (5025310) and STCSM.

References

1. Iijima S (1991) Nature 56:354
2. Zhang XF, Sreekumar TV, Liu T et al (2004) J Phys Chem B 108:16435
3. Terrones M (2003) Annu Rev Mater Res 33:419
4. Rao CNR, Satishkumar BC, Govindaraj A et al (2001) Chemphyschem 2:78
5. Besancon BM, Green PF (2004) Macromol 38:110
6. Li SP, Qin YJ, Shi JH et al (2005) Chem Mater 17:130
7. Weisenberger MC, Grulke EA, Jacques D et al (2003) J Nanosci Nanotech 3:535
8. Yang JW, Hu JH, Wang CC (2004) Macromol Mater Eng 289:828
9. Zhu J, Peng HQ, Macias FR et al (2004) Adv Funct Mater 14:643
10. Blond D, Barron V, Ruether M et al (2006) Adv Funct Mater 16:1608
11. Wang SR, Liang ZY, Liu T et al (2006) Nanotechnology 17:1551
12. Sun YP, Fu KF, Y Lin, Huang WJ (2002) Acc Chem Res 35:1096
13. Zhang L, Kiny VU, Peng HQ et al (2004) Chem Mater 16:2055
14. Liu AH, Honma I, Ichihara M et al (2006) Nanotechnology 17:2845
15. Sun CH, Berg JC (2003) Adv Colloid Interface Sci 105:151
16. Price GJ, Ansari DM (2004) Poly Inter 53:430
17. Montes -Moran MA, Paredes JI, Martinez-Alonso A et al (2002) Macromolecules 35:5085
18. Askin A, Yazici DT (2005) Chromatographia 61:625
19. Pfohl O, Dohrn R (2004) Fluid Phase Equilibr 217:189
20. Papirer E, Brendle E, Ozil F, Balard H (1999) Carbon 37:1265
21. Schultz J, Lavielle L, Martin CJ (1987) Adhesion 23:45
22. Conder JR, Young CL (1979) Physicochemical measurement by gas chromatography. Wiley-Interscience, New York
23. Grob RL (ed) (1995) Modern practice of gas chromatography. Wiley-Interscience, New York
24. Liu LQ, Zhang SA, Hu TJ et al (2002) Chem Phys Lett 359:191
25. Yang D, Hu JH, Wang CC (2006) Carbon 44:316
26. Gao C, Vo CD, Jin YZ, Li WW, Armes SP (2005) Macromolecules 38:8634
27. Kamdem DP, Bose SK, Luner P (1993) Langmuir 9:3039
28. Panzer U, Schreiber HP (1992) Macromolecules 25:3633
29. Bailey RA, Persaud KC (1988) Anal Chim Acta 363:147
30. Planinsek O, Buckton G (2003) J Pharmcaol Sci 92:1286
31. J Schultz K Tsutsumi, Donnent JB (1977) J Colloid Interface Sci 59:272
32. M Shui (2003) Appl Surf Sci 220:359
33. Packham DE (1992) Handbook of adhesion. Longman, London